Robotica (2005) volume 23, pp. 189–196. © 2005 Cambridge University Press
doi:10.1017/S0263574704000645 Printed in the United Kingdom

Dynamic modeling of tip-over stability of mobile manipulators considering the friction effects

R. F. Abo-Shanab and N. Sepehri*

Department of Mechanical and Manufacturing Engineering, The University of Manitoba, Winnipeg, Manitoba (Canada) R3T-5V6

(Received in Final Form: June 12, 2004)

SUMMARY

This paper extends the models developed previously by the authors for simulating tip-over stability of mobile manipulators, to include the friction of the contact between the base and the ground. Thus, the present model takes into account the detailed dynamics of the base that can rock back and forth during the movement of the manipulator, the combined vehicle suspension and ground-tire compliance and, the friction between the wheels and the ground. 'LuGre' tire friction model is employed, which along with the novel method of virtual links transforms the system into a fixed base manipulator with single degree of freedom at each joint. The model is then used to simulate planar movements of a 215B Caterpillar excavator-based log-loader machine. The results are also compared to those obtained by the simplified model, which was developed previously based on the assumption that the friction between the base and the ground is high enough to prevent the base from skidding forward or backward. The results clearly show that the friction properties between the wheels and the ground affect machine stability. Thus, one has to include the frictional effect in order to accurately predict the tip-over behavior of mobile manipulators.

KEYWORDS: Mobile manipulators; Tip-over stability; Dynamic model; Virtual links; LuGre friction model.

1. INTRODUCTION

In many applications such, as space exploration, toxic waste clean up, construction, and forestry, mobile manipulators are required instead of conventional industrial manipulators that are mounted on fixed bases. A typical example of an industrial mobile manipulator is an excavator-based log-loader (see Fig. 1). One issue during the operation of such machines is the proper monitoring and prevention of tip-over. Presently, the operators must face the non-intuitive and exhaustive task of maintaining the machine stability, particularly when handling heavy loads. Although sensor systems are available for some mobile manipulators, such as cranes, that detect whether a static load exceeds the safe operating load, there is no mechanism available that includes dynamic situations. Therefore, the operator must remain alert at all times in order to accomplish the work efficiently and, at the same time protect his/her safety and that of others.

In spite of much research on mobile manipulators, dynamic stability of mobile manipulators in the presence of factors such as flexibility of the contact between the base and the ground, the compliance at the manipulator joints, and the friction between the base and the ground have not been fully explored. For detailed description of the previous relevant studies and a discussion on the results achieved, readers are referred to the previous work by the authors,[1] and the references listed therein. Also, understanding the details of the base movement during the tipping over, can help to define an accurate measure of stability and therefore potentially help to prevent and/or recover from the tipping over. Thus, the general objectives of this work are to: (i) develop a simulation model of tip over motion of mobile manipulators, and (ii) study tip-over mechanisms, and understand various dynamic situations that promote vehicle instability. Within this context, the initial model,[1] although shown to be capable of producing valuable information about the movement of the base, relied on the unrealistic assumption of rigid contact between the base and the ground. The model was then improved to include the flexibility of the contact between the base and the ground.[2] Inclusion of the flexibility, which is due to the suspension and the tires, resulted in a more realistic model. Using this model, it was shown that assuming rigid contact between the base of the mobile manipulator and the ground overestimates the stability and therefore the flexibility of the contact must be considered to more accurately predict the stability and simulate the base motion. The developed simulation model, however, assumed that the friction between the base and the ground is large enough to prevent the manipulator from skidding forward or backward. Furthermore, distinct models had to be used to describe various phases of the dynamics of the vehicle and its manipulator. This form of modeling becomes extremely complicated when applied to three-dimensional motion simulations.

In this paper, the recently developed model is further extended to include the effect of the friction between the wheels and the ground. Here, it is assumed that the wheels of the mobile manipulator are locked in place. Thus, there is no rolling and the friction is only due to the stick-slip motion between the wheels and the ground. The approach taken

* Corresponding author: E-mail: nariman@cc.umanitoba.ca

Fig. 1. Typical excavator-based log-loader.

was to first employ an appropriate coulomb (dry) friction model that is easy to implement, computationally efficient, and characterizes most of the friction phenomena. 'LuGre' friction model[3] was used in this work. LuGre friction model is built upon Dahl friction model,[4] and has been used by others to describe the friction forces between the tire and the road for vehicle control and simulation studies.[5] Next, the novel method of virtual links was applied to cast the resulting problem into a fixed base serial link manipulator with single degree of freedom at each joint. The method of virtual links was presented earlier by Abo-Shanab and Sepehri[6] to facilitate the derivation of the dynamic equations of non-fixed base manipulators. The inclusion of the LuGre friction model also allows the derivation of a single dynamic model to describe the heave, pitch and skid motion as well as lifting up of the base from the ground.

The application of this study is directed at industrial mobile machines that carry human operated hydraulic manipulators. The development here is therefore exemplified with a Caterpillar excavator-based log-loader (see Fig. 1). This machine incorporates many aspects of typical robotic systems and is the basis of most heavy-duty hydraulic machines. Thus, the analysis and the development reported here can be applied to other similar mobile robotic systems. Particularly, this model provides simulation capabilities towards the stability analysis of manipulators mounted on mobile platforms. It also facilitates design of suitable tip over prevention schemes. This is significant since with the introduction of computer control, safety, productivity and lifetime of heavy-duty hydraulic mobile machines could be improved by automatic prediction, prevention and recovering from tip over.

2. DEVELOPMENT OF THE MODEL

The schematic of a planar mobile manipulator is shown in Fig. 2. The base is considered as a rigid body, resting on two wheels that are longitudinally aligned and are modeled using the half car representation with a Kelvin-Voigt spring damping system.[7] The system damping is viscous, below the critical value and invariant with respect to changes of the kinematics configuration. In addition to undergoing heave

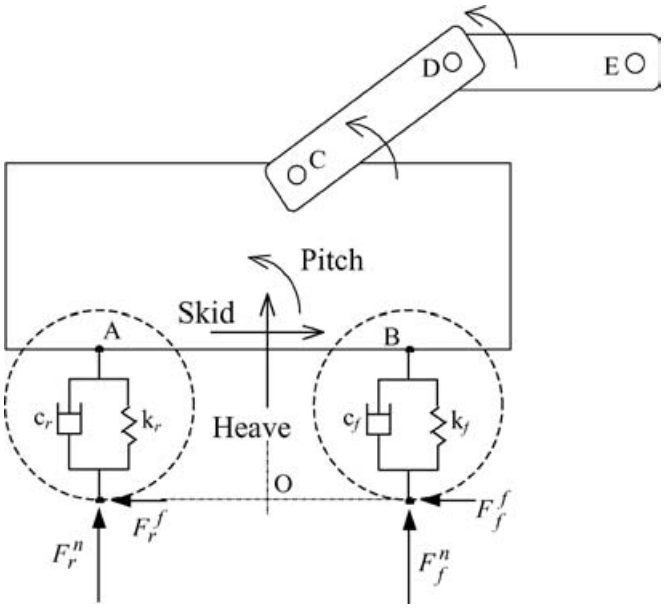

Fig. 2. Schematic diagram of planar mobile manipulator including ground reaction forces.

https://doi.org/10.1017/S0263574704000645 Published online by Cambridge University Press

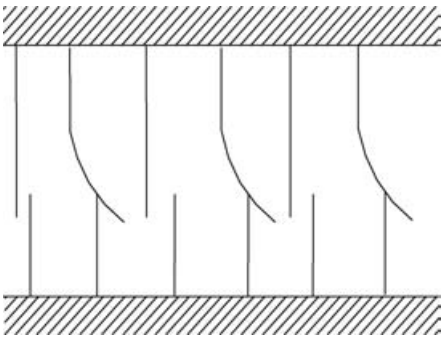

Fig. 3. Friction interface between two surfaces is thought as a contact between bristles. For simplicity the bristles on the lower part are shown as being rigid.[10]

and pitch motions, the base could also skid forward or backward depending on the nature of forces applied to it as well as the friction between the wheels and the ground. With reference to Fig. 2, c and k are the damping and the stiffness coefficients, respectively. F^f and F^n are the friction and normal forces, respectively. The subscripts f and r refer to the front and rear wheels, respectively.

The LuGre friction model is used to model the friction forces between the wheels and the ground. It describes arbitrary steady-state friction characteristics, supports hysteresis behavior due to frictional lag, and gives a varying break-away force depending on the rate of change of the applied force.[8,9] The model is inspired by the bristle interpretation of friction as introduced by Haessig and Friedland[10] and is characterized as the average deflection force of elastic springs (Fig. 3). When a tangential force is applied, the bristles will deflect. If the deflection is sufficiently large, the bristles start to slip over each other. Using the LuGre friction model, the force, F^f, generated from the bending of the bristles is described as:

$$F^f = (\sigma_o z + \sigma_1 \dot{z} + \sigma_2 \nu) F^n \tag{1}$$

where σ_o is the normalized lumped stiffness, σ_1 is the normalized lumped damping, σ_2 is the normalized viscous relative damping, F^n is the normal force, and ν is the relative velocity between the two surfaces in contact. The average deflection of the bristles is denoted by z and is modeled by the following relation:

$$\dot{z} = \nu - \frac{\sigma_o |\nu|}{\eta(\nu)} z \tag{2}$$

Function $\eta(\nu)$ contains information about the velocity dependence of friction. It is positive and depends on many factors such as material properties, lubrication, and temperature:

$$\eta(\nu) = \mu_c + (\mu_s - \mu_c) e^{-|\nu/\nu_s|^\alpha} \tag{3}$$

In (3), μ_c is the Coulomb friction coefficient, μ_s is the static friction coefficient and ν_s is the Stribeck velocity, which helps to define the velocity dependence of friction. α is an application-dependent exponent. Canudas de Wit and Tsiotras[3] suggested $\alpha = 0.5$ for modeling the friction between the tires and the ground.

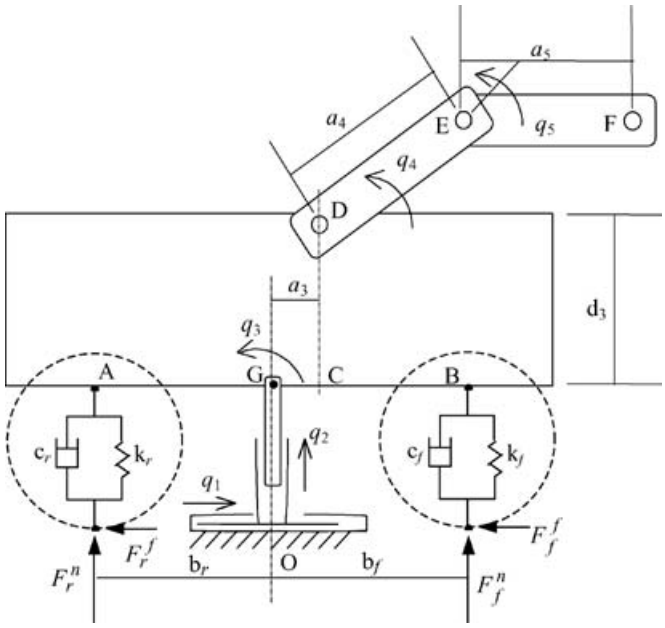

Fig. 4. Schematic diagram of planar mobile manipulator including the virtual links, suspension and LuGre friction forces.

To derive the dynamic equations of the entire machine, two virtual links[6] with prismatic joints are added to represent the horizontal (skid) and vertical (heave) movements, q_1 and q_2, of the base (see Fig. 4). The second virtual link is connected to the base by a revolute joint characterizing the pitch movement of the base, q_3. Denavit-Hartenberg (DH) coordinate systems are assigned to the manipulator's links as shown in Fig. 5. The manipulator link coordinate parameters are listed in Table I.

The dynamic equations are derived based on the Lagrange formulation:

$$\boldsymbol{\tau} = \mathbf{M}(\mathbf{q})\ddot{\mathbf{q}} + \mathbf{C}(\mathbf{q}, \dot{\mathbf{q}}) + \mathbf{G}(\mathbf{q}) + \boldsymbol{\tau}_{ext} \tag{4}$$

where $\mathbf{q} = \{q_1, q_2, \ldots, q_5\}^T$, $\dot{\mathbf{q}}$ and $\ddot{\mathbf{q}}$ are vectors of the joint variables, velocities and accelerations, $\boldsymbol{\tau}(t) = \{\tau_1, \tau_2, \ldots, \tau_5\}^T$ is the generalized force vector applied at the joints. $\boldsymbol{\tau}_{ext} = \{\boldsymbol{\tau}_{ext_1}, \boldsymbol{\tau}_{ext_2}, \boldsymbol{\tau}_{ext_3}, \boldsymbol{\tau}_{ext_4}, \boldsymbol{\tau}_{ext_5}\}^T$ is the vector of external forces due to ground reaction forces.

The elements of the 5×5 inertial acceleration-related symmetric matrix, $\mathbf{M}(\mathbf{q})$, are derived using the following

Table I. Link coordinate parameters.

Link	θ_i	d_i	A_i	α_I	Variables
1	$\pi/2$	q_1	0	$\pi/2$	q_1
2	$\pi/2$	q_2	0	$\pi/2$	q_2
3a	q_3	0	A_3	$-\pi/2$	q_3
3	0	d_3	0	$\pi/2$	–
4	q_4	0	a_4	0	q_4
5	q_5	0	a_5	0	q_5

https://doi.org/10.1017/S0263574704000645 Published online by Cambridge University Press

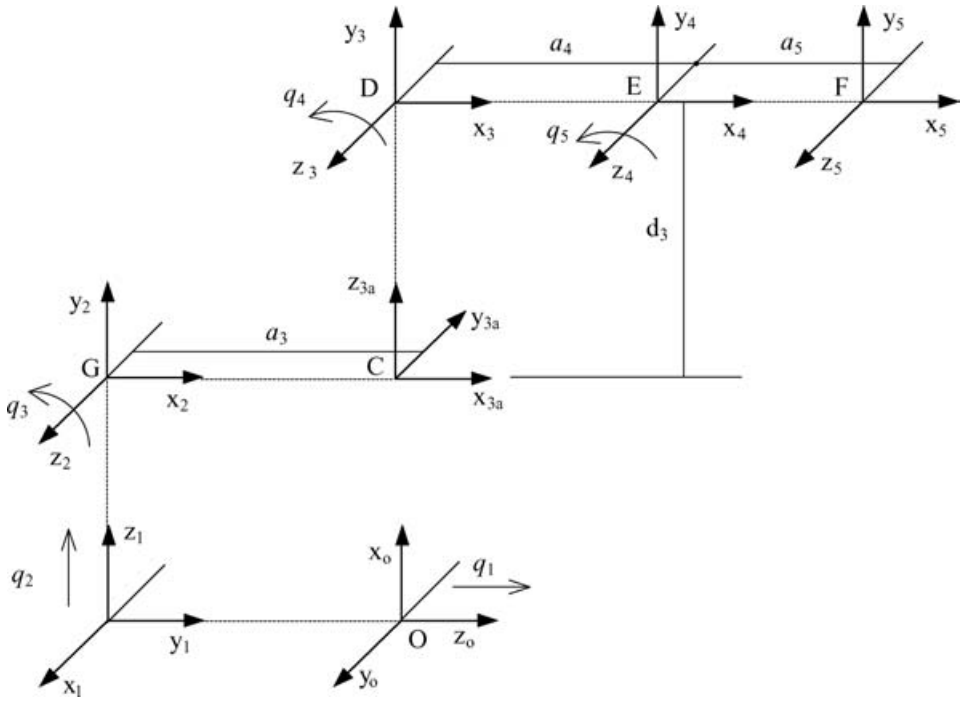

Fig. 5. Link coordinate systems pertaining to Fig. 4.

relations:

$$M_{ij} = Trace\left\{\mathbf{\Delta}_i\left[\sum_{p=j}^{5}\mathbf{T}_p\mathbf{J}_p\mathbf{T}_p^T\right]\mathbf{\Delta}_j^T\right\} \quad (j \geq i)$$
$$M_{ji} = M_{ij} \quad (i < j) \tag{5}$$

The elements of the Coriolis and centrifugal force vector $\mathbf{C}(\mathbf{q}, \dot{\mathbf{q}}) = \{c_1, c_2, \ldots, c_5\}^T$ are determined as follows:

$$C_i = \sum_{j=1}^{5}\sum_{i=1}^{5} c_{ijk}\,\dot{q}_j\,\dot{q}_k$$

where

$$c_{ijk} = Trace\left\{\mathbf{\Delta}_i\left[\sum_{p=j}^{5}\mathbf{T}_p\mathbf{J}_p\mathbf{T}_p^T\right]\mathbf{\Delta}_j^T\mathbf{\Delta}_k^T\right\} \quad (j \geq i,\ j \geq k)$$
$$c_{ikj} = c_{ijk}$$
$$c_{kji} = -c_{ijk} \quad (j < i,\ j < k) \tag{6}$$

The elements of the gravitational force vector $\mathbf{G}(\mathbf{q}) = \{G_1, G_2, \ldots, G_5\}^T$ are:

$$G_i = -(\mathbf{g}^T; 0)\mathbf{\Delta}_i\left[\sum_{p=i}^{5} m_p\mathbf{T}_p\left(\mathbf{r}_p^p; 1\right)\right] \tag{7}$$

where $\mathbf{g}$ is the gravitational acceleration vector in base coordinate frame, $\mathbf{r}_i^i$ is the position vector of mass center of link i in coordinate frame i. In equations (5), (6) and (7), $\mathbf{T}_i$ is the homogeneous transformation matrix from coordinate frame i to the base coordinate frame. $\mathbf{J}_i$ is defined as

$$\mathbf{J}_i = \begin{bmatrix} \mathbf{J}_i^i + m_i\mathbf{r}_i^i\mathbf{r}_i^{iT} & m_i\mathbf{r}_i^i \\ m_i\mathbf{r}_i^{iT} & m_i \end{bmatrix}$$

where $\mathbf{J}_i^i$ is a 3×3 inertial matrix of link i about its mass center in coordinate frame i and m_i is the mass of link i. $\mathbf{\Delta}_i$ is a differential operator; it is defined as:[11]

$$\mathbf{\Delta}_i = \begin{bmatrix} \lambda_i\tilde{\mathbf{z}}_{i-1} & [\lambda_i\tilde{\mathbf{P}}_{i-1} + (1-\lambda_i)\mathbf{I}]\mathbf{z}_{i-1} \\ \mathbf{0} & 0 \end{bmatrix} \tag{8}$$

where $\mathbf{z}_i$ is z-*axis* of coordinate frame i, and $\mathbf{p}_i$ is the position vector of the origin of coordinate frame i with respect to the base coordinate. $\lambda_i = 1$ for revolute joints; $\lambda_i = 0$ for prismatic joints. $\mathbf{I}$ is the identity matrix. The symbol '~' in (8) denotes a skew symmetric matrix with zero diagonal values. For example, given a vector $\mathbf{u} = \{u_x, u_y, u_z\}^T$, $\tilde{\mathbf{u}}$ is defined as:

$$\tilde{\mathbf{u}} = \begin{bmatrix} 0 & -u_z & u_y \\ u_z & 0 & -u_x \\ -u_y & u_x & 0 \end{bmatrix}$$

The normal forces, F_f^n and F_r^n, and friction forces, F_f^f and F_r^f, at the rear and the front wheels, are calculated as follows:

$$F_r^n = -k_r(q_2 - b_r\sin q_3 - x_o) - c_r(\dot{q}_2 - b_r\cos q_3\dot{q}_3) \tag{9}$$
$$F_f^n = -k_f(q_2 + b_f\sin q_3 - x_o) - c_f(\dot{q}_2 + b_f\cos q_3\dot{q}_3) \tag{10}$$

https://doi.org/10.1017/S0263574704000645 Published online by Cambridge University Press

$$F_r^f = (\sigma_{or} z_r + \sigma_{1r}\dot{z}_r + \sigma_{2r}\dot{x}_A)F_r^n \tag{11}$$

$$F_f^f = (\sigma_{of} z_f + \sigma_{1f}\dot{z}_f + \sigma_{2f}\dot{x}_B)F_f^n \tag{12}$$

where x_o is the undeformed length of the springs characterizing the suspension. Further,

$$\dot{z}_r = \dot{x}_A - \frac{\sigma_{or}|\dot{x}_A|}{\eta_r(\dot{x}_A)} z_r \tag{13}$$

and

$$\dot{z}_f = \dot{x}_B - \frac{\sigma_{of}|\dot{x}_B|}{\eta_f(\dot{x}_B)} z_f \tag{14}$$

where

$$\eta_r(\dot{x}_A) = \mu_{c_r} + (\mu_{s_r} - \mu_{c_r})e^{-\left|\frac{\dot{x}_A}{v_{S_r}}\right|^{0.5}} \tag{15}$$

$$\eta_f(\dot{x}_B) = \mu_{c_f} + (\mu_{s_f} - \mu_{c_f})e^{-\left|\frac{\dot{x}_B}{v_{S_f}}\right|^{0.5}} \tag{16}$$

Then

$$\begin{aligned}
\tau_{ext_1} &= F_f^f + F_r^f \\
\tau_{ext_2} &= -F_f^n - F_r^n \\
\tau_{ext_3} &= F_r^f(q_2 - b_r sinq_3) + F_f^f(q_2 + b_f sinq_3) \\
&\quad + F_r^n b_r cosq_3 - F_f^n b_f cosq_3 \\
\tau_{ext_4} &= 0 \\
\tau_{ext_5} &= 0
\end{aligned} \tag{17}$$

3. SIMULATION STUDIES

The developed model is now applied to the Caterpillar log-loader shown in Fig. 1. The machine is a mobile three degree-of-freedom manipulator with a grapple for holding and handling objects such as trees. The whole machine can move forwards or backwards. The upper structure of the machine rotates on the carriage by a 'swing' hydraulic motor through a gear train. 'Boom' and 'stick' are the two other links, which together with the 'swing', serve to position the implement (see also the inset of Fig. 6). Boom and stick are operated through hydraulic cylinders. The cylinders and the swing motor are activated by means of pressure and flow through the main valves. Modulation of the oil flow in the main valves is presently controlled by the pilot oil pressure through manually operated pilot control valves. The equations governing the hydraulic actuation system are given in details in reference [1] and thus are not repeated here.

Here, the swing is locked. Thus, the movement of the implement is limited to a planar motion. The kinematic parameters are $a_3 = 1.5$ m, $a_4 = 5.2$ m, $a_5 = 1.8$ m, $b_f = 2.5$ m, $b_r = 2.5$ m, and $d_3 = 1.5$ m (see Figs. 4 and 5). The dynamic parameters are listed in Table II. The parameters indicating the flexibility between the ground and the base, are chosen as $k_1 = k_2 = 35 \times 10^5\, N/m$ and $B_1 = B_2 = 15 \times 10^4\, Ns/m$. These values provide a natural frequency of ≈ 3.5 Hz and a damping ratio of ≈ 0.47 in the vertical direction, which change with the manipulator configuration and payload.

The friction coefficients were chosen as $\mu_{s_f} = \mu_{s_r} = 0.05$ and $\mu_{c_f} = \mu_{c_r} = 0.03$. The values of other parameters used in LuGre model were selected as $\sigma_{o_f} = \sigma_{o_r} = 40$ l/m,

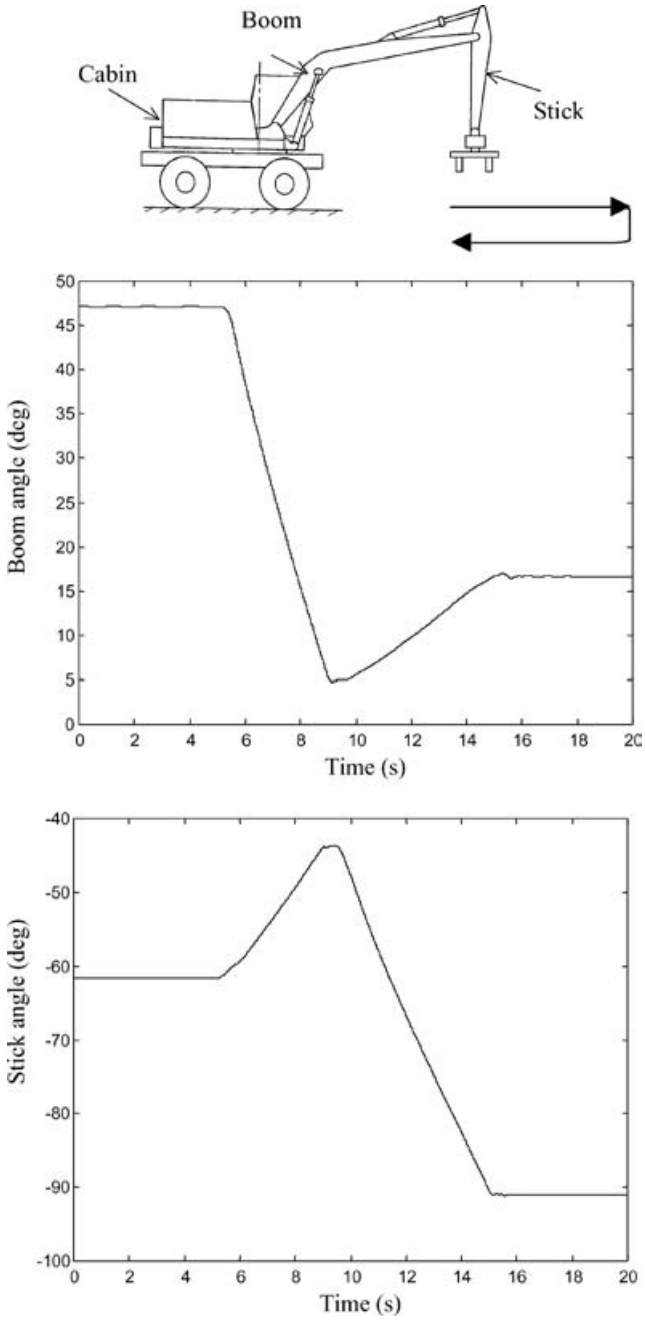

Fig. 6. Manipulator movement during a pick-and-place operation.

Table II. Dynamic Parameters.

	Mass (kg)	Mass moment of inertia (kg m^2)	Center of gravity (x, y, z) m	Coordinate frame
Base	12,000	90,523	(−2.0, −0.6, 0.0)	{x$_3$ y$_3$ z$_3$}
Boom	1,830	15,500	(−2.9, 0.2, 0.0)	{x$_4$ y$_4$ z$_4$}
Stick	688	610	(−0.9, 0.1, 0.0)	{x$_5$ y$_5$ z$_5$}

https://doi.org/10.1017/S0263574704000645 Published online by Cambridge University Press

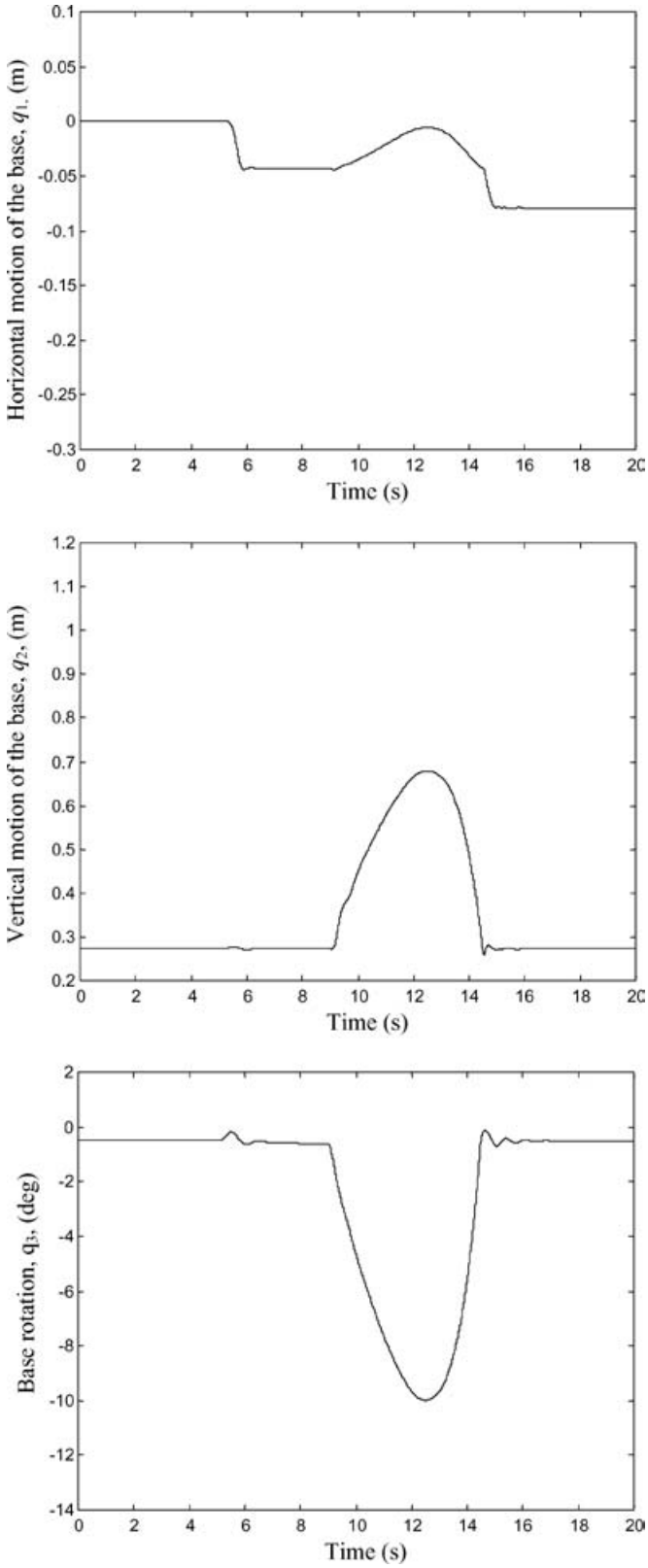

Fig. 7. Motion of base during the pick-and-place operation.

$\sigma_{1_f} = \sigma_{1_r} = 4.9487$ s/m, $\sigma_{2_f} = \sigma_{2_r} = 0.0018$ s/m, and $v_{s_f} = v_{s_r} = 12.5$ m/s. These values were used by Canudas de Wit and Tsiotras[3] for tire friction models and gave results that matched reasonably well with their experimental data and are therefore adopted here.

The simulated task is to have the machine end-effector to perform a pick-and-place operation. In this task, the end-effector starts from a position close to the base carrying a 5000 kg load. The base is initially stable. The manipulator extends the end-effector to a possible 'dumping position' far from the base. Fig. 6 shows the corresponding motions of the manipulator's links (i.e., boom and stick). Fig. 7 shows the movement of the base described by horizontal and vertical movements of, and its rotation about point G (see Fig. 4). Fig. 8 shows the vertical movements of the front (point B) and rear (point A) edges of the base. Note that the dotted lines represent the undeformed location of the spring representing the flexibility between the base and the ground. Any displacement of the edges above the dotted lines denotes the lifting up of the edge. As it is seen, the front edge did not lift off, whereas, the rear edge lifted up for a period of time, but return without causing the whole machine to overturn. Fig. 9 shows the skidding of the base (represented by the movement of the front edge point B) as well as the rotation of the base. With reference to this figure, it is seen that the base moves horizontally, with respect to the ground mainly on two occasions; when the manipulator starts to move, and when the base rocks over the edge A and hit the ground. The whole task moved the base ≈ 75 mm. Fig. 10 shows the

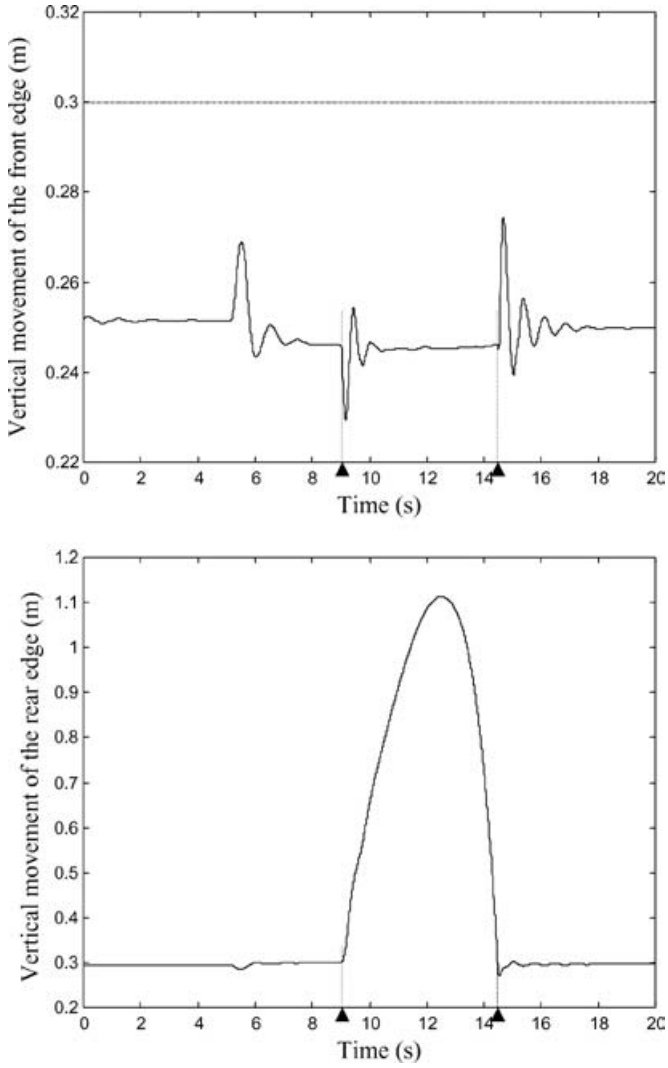

Fig. 8. Vertical movements of the front and the rear edges of the base during the pick-and-place operation.

https://doi.org/10.1017/S0263574704000645 Published online by Cambridge University Press

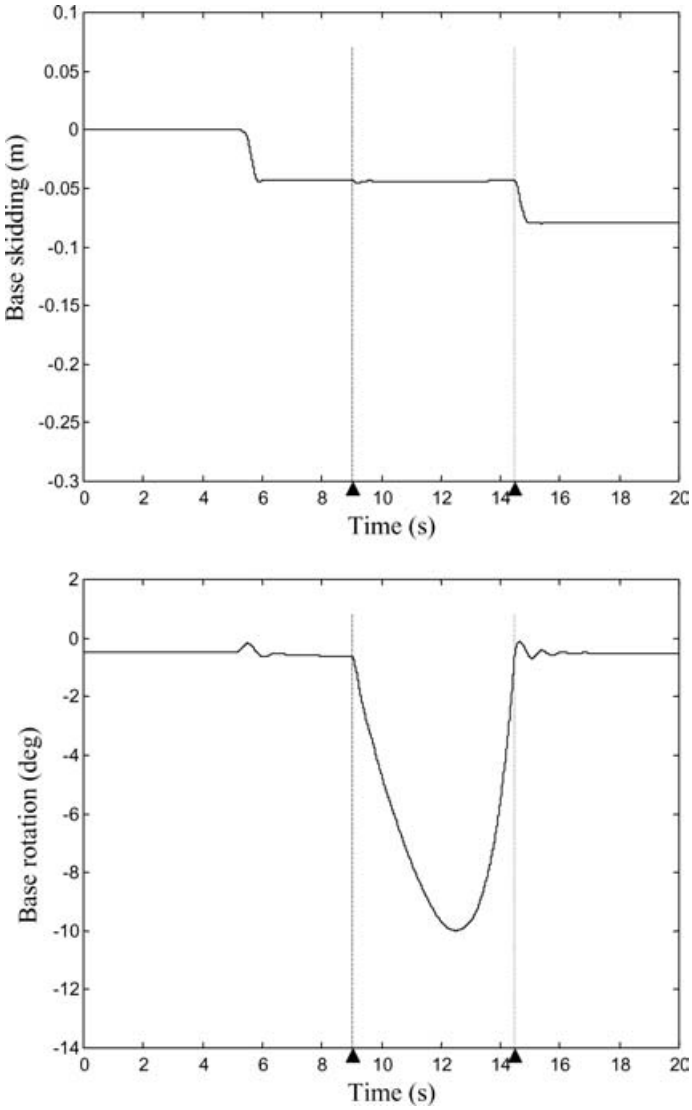

Fig. 9. Base rotation and skidding during the pick-and-place operation.

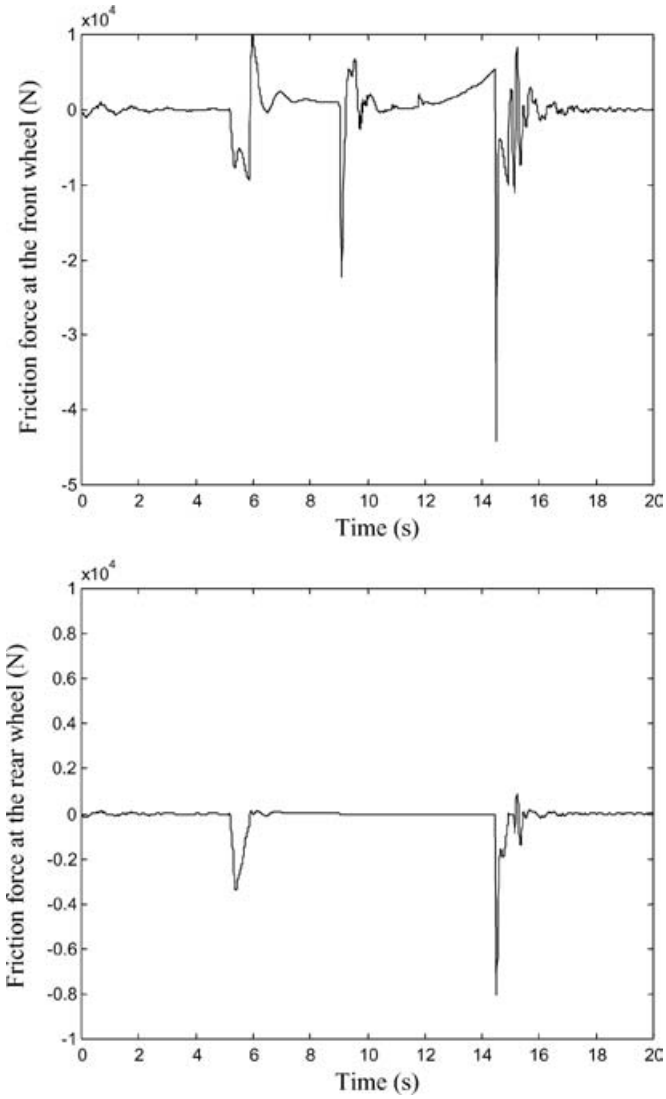

Fig. 10. Friction forces at the front and rear wheels.

values of the frictional forces at the front and rear wheels of the vehicle, which have been determined by the LuGre model of friction.

The developed model is also compared to the simplified model, developed in the previous work,[2] based on the assumption that the friction between the base and the ground is high enough to prevent the base from skidding forward or backward. Fig. 11 shows the simulation results using the two models. It is seen that the simplified model underestimates the stability of the manipulator given the same task. So, one has to include the frictional effects to more accurately characterize mobile manipulators during a tip-over.

Finally, the simulation model is further used to investigate the effect of the variation of the frictional properties between the base and the ground on the machine tip over stability. Fig. 12 shows that, for the simulation reported here, reducing the friction between the base and the ground improves the machine stability up to a certain limit below which, the machine starts to also skid noticeably during the tipping over, causing the machine to become less stable. This is seen from Fig. 12 where at $t \approx 9$ s, the machine starts to slide

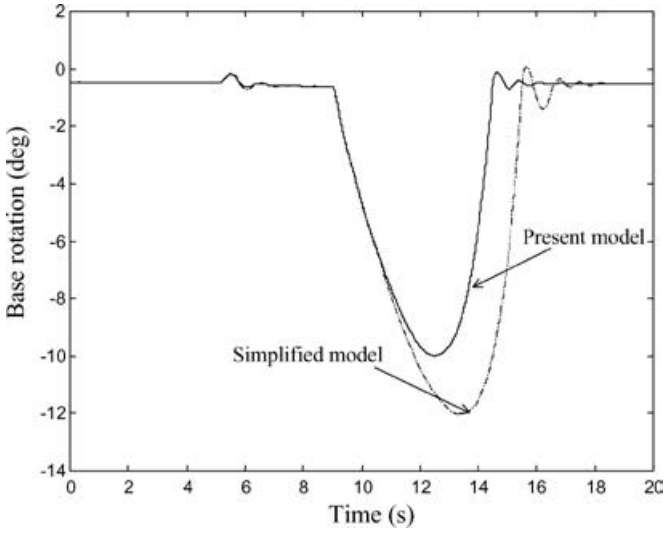

Fig. 11. Base rotation using different friction models.

https://doi.org/10.1017/S0263574704000645 Published online by Cambridge University Press

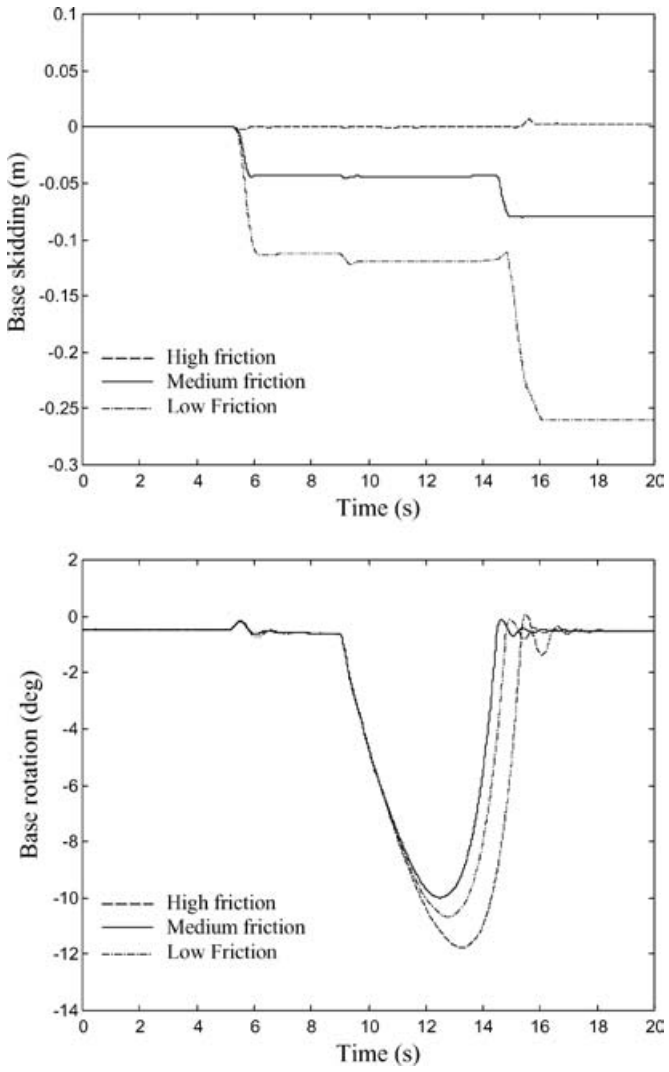

Fig. 12. Base movement (skid and rotation) using LuGre model with different friction coefficient values: high friction: $\mu_s = 0.9$, $\mu_d = 0.5$; medium friction: $\mu_s = 0.005$, $\mu_d = 0.03$; low friction: $\mu_s = 0.02$, $\mu_d = 0.012$.

significantly for low friction. This motion negatively affects the machine stability.

4. CONCLUSIONS

In this paper, a dynamic model for a two-link planar mobile manipulator was developed to study and analyze the tip over motion of mobile manipulators due to the movement of their arms. The model takes into account the detailed dynamics of the base that can rock back and forth, the flexibility and the friction of the contact between the base and the ground, and the interaction between the vehicle and the manipulator including the payload. The 'LuGre' tire friction model was employed to calculate the friction forces between the wheels and the ground and predict the skidding phenomenon. The contact between the base and the ground was considered as a multi-degree-of-freedom joint, and the method of virtual links was used to formulate the problem into a fixed base serial-link manipulator with single degree of freedom at each joint. This process allowed the derivation of differential equations that describe the dynamics of the entire system, to be conducted in a more systematic and easier manner.

A Caterpillar excavator-based hydraulic machine was chosen to demonstrate the development presented in this paper. This machine incorporates many aspects of typical robotic systems and is similar to many heavy-duty hydraulic equipment units. Thus, the analysis, development, and results reported in this paper can be applied to other similar mobile robotic systems.

Simulation results were presented to substantiate the model development here. The results of the developed model were also compared to those obtained by a simplified model developed previously by the authors. It was shown that the simplified model underestimates the stability, therefore, the friction effect should be included to accurately investigate the stability of mobile manipulators. Finally, the developed model was used to investigate the effect of the variation of the frictional properties between the wheels and the ground on the manipulator's stability. The simulations reported here showed that reducing the friction between the base and the ground increases the machine stability up to a certain limit, below which the machine starts to also skid significantly during the tipping over, causing the machine to become less stable.

References

1. R. F. Abo-Shanab and N. Sepehri, "On Dynamic Stability of Manipulators Mounted on Mobile Platforms," *Robotica* **19**, Part 4, 439–449 (2001).
2. R. F. Abo-Shanab and N. Sepehri, "The Effect of Base Compliance on the Dynamic Stability of Mobile Manipulators," *Robotica* **20**, Part 1, 607–613 (2002).
3. C. Canudas de Wit and P. Tsiotras, "Dynamic Tire Friction Models for Vehicle Traction Control," *Proceedings 38th Conference on Decision and Control*, Phoenix, AZ (1999) pp. 3746–3751.
4. P. R. Dahl, "Solid Friction Damping of Mechanical Vibrations," *AIAA Journal* **14**, 1675–1682 (1976).
5. X. Claeys, J. Yi, R. Horowitz, L. Alvarez and C. Canudas de Wit, "A Dynamic Tire/Road Friction Model for 3D Vehicle Control and Simulation," *Proceedings of the IEEE Intelligent Transportation Systems Conference*, Oakland, CA (2001) pp. 483–488.
6. R. F. Abo-Shanab, N. Sepehri and Q. Wu, "On Dynamic Modeling of Robot Manipulators: the Method of Virtual Links," *Proceedings of ASME Design Engineering Technical Conference*, Montreal, Canada (2002) paper DETC2002/MECH-34225.
7. U. O. Akpan and M. R. Kujath, "Sensitivity of a Mobile Manipulator Response to System Parameters," *ASME Journal of Vibration and Acoustics* **120**, 156–163 (1998).
8. C. Canudas de Wit, H. Olsson, K. Astrom and P. Lischinsky, "A New Model for Control of Systems with Friction," *IEEE Transactions on Automatic Control* **40**, 419–425 (1995).
9. B. Armestrong-Helouvery, P. Dupont and C. Canudas de Wit, "A Survey of Models, Analysis Tools and Compensation Methods for the Control of Machines with Friction," *Automatica* **30**, 1083–1138 (1994).
10. D. A. Haessig and B. Friedland, "On the Modeling and Simulation of Friction," *ASME Journal of Dynamic Systems, Measurement, and Control* **113**, 354–362 (1991).
11. M. M. Sallam, R. F. Abo-Shanab and A. A. Nasser, "Modified Methods for Dynamic Modeling of Robot Manipulators," *Proceedings ASME Design Engineering Technical Conference*, Atlanta, GA (1998) Paper DETC98/MECH5860.

https://doi.org/10.1017/S0263574704000645 Published online by Cambridge University Press